

J. Mlynar, M. Imrisek, V. Weinzettl, M. Odstreil, J. Havlicek, F. Janky,
B. Alper, A. Murari and JET EFDA contributors

Introducing Minimum Fisher Regularisation Tomography to Bolometric and Soft X-ray Diagnostic Systems of the COMPASS Tokamak

“This document is intended for publication in the open literature. It is made available on the understanding that it may not be further circulated and extracts or references may not be published prior to publication of the original when applicable, or without the consent of the Publications Officer, EFDA, Culham Science Centre, Abingdon, Oxon, OX14 3DB, UK.”

“Enquiries about Copyright and reproduction should be addressed to the Publications Officer, EFDA, Culham Science Centre, Abingdon, Oxon, OX14 3DB, UK.”

The contents of this preprint and all other JET EFDA Preprints and Conference Papers are available to view online free at www.iop.org/Jet. This site has full search facilities and e-mail alert options. The diagrams contained within the PDFs on this site are hyperlinked from the year 1996 onwards.

Introducing Minimum Fisher Regularisation Tomography to Bolometric and Soft X-ray Diagnostic Systems of the COMPASS Tokamak

J. Mlynar¹, M. Imrisek², V. Weinzettl¹, M. Odstrcil,^{1,2} J. Havlicek^{1,3}, F. Janky^{1,3},
B. Alper⁴, A. Murari⁵ and JET EFDA contributors*

JET-EFDA, Culham Science Centre, OX14 3DB, Abingdon, UK

¹*Institute of Plasma Physics AS CR, Association EURATOM-IPP.CR, Za Slovankou 3,
CZ-182 00 Prague 8, Czech Republic*

²*Faculty of Nuclear Sciences and Physical Engineering, CTU Prague, Association EURATOM-IPP.CR,
Brehova 8, CZ-115 19 Prague 1, Czech Republic*

³*Faculty of Mathematics and Physics, Charles University, Prague, Association EURATOM-IPP.CR,
V Holesovickach 2, CZ-180 00 Prague 8, Czech Republic*

⁴*EURATOM-CCFE Fusion Association, Culham Science Centre, OX14 3DB, Abingdon, Oxon, UK*

⁵*Consorzio RFX, Association EURATOM-ENEA sulla Fusione, I-35127, Padova, Italy*

** See annex of F. Romanelli et al, "Overview of JET Results",
(23rd IAEA Fusion Energy Conference, Daejeon, Republic of Korea (2010)).*

Preprint of Paper to be submitted for publication in Proceedings of the
High Temperature Plasma Diagnostics (HTPD) 2012, Monterey, California, USA.

7th May 2012 - 10th May 2012

ABSTRACT

The contribution focuses on plasma tomography via the Minimum Fisher Regularisation (MFR) algorithm applied on data from the recently commissioned tomographic diagnostics on the COMPASS tokamak. The MFR expertise is based on previous applications at Joint European Torus (JET), as exemplified in a new case study of the plasma position and Zeff analyses based on JET SXR tomographic reconstruction. Subsequent application of the MFR algorithm on COMPASS AXUV bolometric data disclosed a peaked radiating region near the limiter, and clearly allowed for a high resolution plasma positioning independent of the magnetic diagnostics. Moreover, its time evolution indicates transient plasma cooling following a radial plasma shift. In SXR data, MFR demonstrated that a proper calibration of the cameras on an X-ray source would be required.

1. THE MINIMUM FISHER REGULARISATION

Plasma tomography allows reconstructing 2D plasma emissivity distribution from the plasma projections, i.e. from the line integrated radiation measurements. However, in fusion research the plasma projections are sparse due to engineering constraints and, moreover, the inverse reconstruction represents an ill-conditioned task, with a high risk of overfitting leading to artifacts in the resulting emissivity pattern. In order to avoid the artifacts, regularisation algorithms are applied which implement a-priori information (constraints), in particular the expected smoothness of the emissivity [1].

In the Minimum Fisher Regularisation [2] (MFR) the constraint is introduced by minimizing

$$\Lambda_{MF} = \frac{1}{2} \chi^2 + \alpha I_F, \quad (1)$$

where χ^2 is the goodness-of-fit parameter, α is a regularisation (smoothing) parameter and the Fisher information I_F is defined

$$I_F = \int \frac{(\nabla g)^2}{g} dS, \quad (2)$$

where g represents the reconstructed emissivity distribution. In MFR, plasma emissivity is found for a discrete set of rectangular pixels, so that the relationship between the line integrated data and emissivity can be discretised as follows:

$$f_i = \sum_j T_{ij} g_j + \zeta_i, \quad (3)$$

where f_i represents the line integrated data along individual chords, T_{ij} the contribution matrix reflecting the geometric setup of the pixels and the chords, and ζ_i the unknown errors. The subsequent reconstruction process is based on a Philips-Tikhonov regularisation. Notice that a good estimate of expected errors in data is instrumental for the control of the resulting smoothness,

which is set iteratively to satisfy the target value of χ^2 . As a novel and significant physical constraint, the anisotropic smoothness with respect to the magnetic flux surfaces was introduced: $(\nabla g)^2 \approx gHg$, $H = B_P^T e^\eta B_P + B_\perp^T e^{-\eta} B_\perp$ where B_P and B_\perp correspond to numerical differentiation matrices acting parallel and perpendicular to the magnetic flux surfaces, respectively. Notice that the anisotropy factor $\eta > 0$ enforces preferential smoothness along the magnetic flux surfaces, allowing for steeper gradients in the radial profile of the emissivity reconstruction. Non-negativity and zero border constraints were also implemented [3].

High temporal resolution of SXR and AXUV diagnostics offers an important asset for plasma tomography. In this respect, the MFR algorithm is advantageous due to its short calculation times.³ For example, the plasma position coordinates based on the centre of mass of the emissivity can be readily determined independently of magnetic measurements. Besides, the reconstructed emissivity evolution can be decomposed into spatial and temporal eigenvectors – topos v_i and chronos u_i – and their corresponding amplitude s_i by SVD (the Singular Value Decomposition)²:

$$g(r, t) = \sum_i s_i v_i(r) u_i(t) \quad (4)$$

The SVD decomposition filters out the noise and it also helps to visualise significant events, as will be exemplified in section IV.

2. THE JET SXR TOMOGRAPHY CASE STUDY

At Joint European Torus (JET), the MFR algorithm was optimised and thoroughly tested for the current Soft X-Ray (SXR) diagnostics setup [3]. The JET SXR diagnostics consist of 30 vertical chords (pinhole camera V) shielded by 250mm Be foil, and 17 horizontal chords (collimated cameras S4) shielded with 350mm Be foil. Due to different construction of the V and S4 cameras, their spectral response to SXR radiation is different. In addition to recently published results [3,4] the optimised MFR was used to follow the plasma core position via the centre of mass of the reconstructed MFR emissivity [5].

A convincing agreement between position determined by the MFR and by standard magnetic diagnostics was demonstrated except some transitional effects, e.g. due to plasma heating, which deserves further studies, see Fig.1. Second, the MFR also allowed for correct estimate of the effective charge Z_{eff} in the core plasma from SXR profile reconstruction under the assumption that the plasma SXR emissivity is due to bremsstrahlung only.⁶ As follows from Fig.2, the assumption is valid for $\psi_{norm} < 0.3 \div 0.4$.

3. THE COMPASS TOKAMAK TOMOGRAPHIC DIAGNOSTICS

After its reinstallation in Prague, the COMPASS tokamak ($R=0.56\text{m}$, $a=0.18\text{m}$, $B_T=2\text{T}$, ITER-like plasma geometry) has been so far operating in the inner limiter regime, with a new plasma position feedback system and new 2x 300kW neutral beam heating injectors. Its tomographic diagnostics,

commissioned in 2011, consists of AXUV bolometers and SXR windowless photodiodes. At present, 6 pinhole AXUV cameras provide line integrated data from 20 channels each (see fig. 3). The AXUV spectral sensitivity covers a broad energy range from 7eV up to 6keV. In SXR, each pinhole camera consists of 35 channels, with the photodiodes shielded by 5 μ m Be foil. Their spectral sensitivity corresponds to energies from approx. 500eV up to 20keV. Both tomographic diagnostics feature high temporal resolution, at present their data are acquired with sampling frequency 2 MHz [7].

4. FIRST EXPERIMENTAL RESULTS OF THE MFR TOMOGRAPHY AT COMPASS

At JET, the advantages of anisotropic smoothness in MFR were clearly demonstrated.³ However, the magnetic flux reconstruction is not available at COMPASS so far. Therefore, pre-form circular flux surfaces were used in the MFR tomographic reconstructions instead. The outermost circle was used as the border constrained to zero emissivity (see fig.3). These constraints proved efficient, both the convergence and retrofit improved compared to the free-form MFR tomography.

The MFR reconstruction of the COMPASS AXUV data clearly allowed identifying the inner limiter region as the main source of the radiation, see Fig. 3. Subsequently, the retrofit (i.e. comparison of real signals with expected signals due to eq. 3, provided that errors ζ_i are negligible) indicated several cases of mismatch in camera sensitivities and positions. Based on these findings, it is planned to determine precise AXUV geometry in-situ by a movable light source. Next, performance of MFR in COMPASS plasma positioning was studied, see Fig.4. The plasma position is determined as the centre of mass of the reconstructed emissivity [4]. In the COMPASS Pulse No: 2648, the radial plasma position was intentionally shifted inwards (i.e. to the high field side, HFS) by 10mm at 1.04s in order to validate the feedback plasma position control. The radial shift is clearly seen in both magnetic and AXUV reconstructions. However, the AXUV centre of mass is substantially offset towards HFS due to strong radiating interaction of the edge plasma with the inner limiter, and consequently it shows a less important radial shift. In the vertical direction, the AXUV position surprisingly indicates a more stable average plasma position than the magnetic data.

Application of the Singular Value Decomposition (SVD) on the evolution of the reconstructed AXUV emissivity clearly visualised an interesting consequence of the shift in the radial plasma position, see Fig.5. While the third topos corresponds to the change of the plasma position itself, the fourth topos demonstrates transient plasma edge cooling combined with the limiter radiation increase. The first and the second topos, which correspond to the base emissivity distribution and the periodic (MHD) plasma oscillation, are not shown.

The MFR reconstruction of the COMPASS SXR data clearly identifies the hot peaked central region, limited typically to $\psi_{norm} > 0.4$. However, the MFR would not converge to a desirable value of the goodness-of-fit parameter χ^2 at COMPASS so that the tomography result is overfitted (too noisy). This first MFR results indicate that the SXR diagnostic cameras should be carefully calibrated on an X-ray source.

CONCLUSIONS

The MFR tomography was successfully practiced on novel SXR studies at JET and subsequently it was applied on new COMPASS data. At JET, the SXR data were analysed by the MFR algorithm in order to validate plasma position and to estimate the plasma effective charge within the region of prevailing bremsstrahlung. At COMPASS, MFR on AXUV data correctly identified plasma position changes; moreover, redistribution of radiation due to plasma cooling was disclosed. The algorithm proved to provide robust and rapid response, and its performance indicated the required future amendments of the COMPASS tomography diagnostics. In particular, to foster the AXUV tomography, the setup geometry (etendue and positions) of the cameras need to be precisely measured in order to improve performance of the tomographic inversion. In the case of the COMPASS SXR diagnostics, a relative calibration of the Be shielded channels on an X-ray source is planned in order to achieve the MFR convergence.

ACKNOWLEDGEMENTS

This work, carried out under the European Fusion Development Agreement, was supported by the European Communities and the contributing Associations. Support from GA CR grants GA 202/09/1467 and GA P205/10/2055, as well as by the MSMT grant #LG11018 is acknowledged. The views and opinions expressed herein do not necessarily reflect those of the European Commission.

REFERENCES

- [1]. L.C. Ingesson, B. Alper, B.J. Peterson, and J.-C. Vallet, *Fusion Science Technology* **53**, 528 (2008).
- [2]. M. Anton, H. Weisen, M.J. Dutch, W. Linden, F. Buhlmann, R. Chavan, B. Marletaz, P. Marmillod, and P. Paris, *Plasma Physics and Controlled Fusion* **38**, 1849 (1996).
- [3]. M. Odstrcil, J. Mlynar, T. Odstrcil, B. Alper, A. Murari and JET EFDA Contributors, submitted to *Nuclear Instruments and Methods* (2012).
- [4]. J. Mlynar, S. Coda, A. Degeling, B.P. Duval, F. Hofmann F, T. Goodman, J.B. Lister, X. Llobet and H. Weisen, *Plasma Physics and Controlled Fusion* **45**(2) 169-180(2003)
- [5]. J. Mlynar, M. Odstrcil, M. Imrisek, B. Alper, C. Giroud, A. Murari, and JET EFDA Contributors, *Contributed Papers 38th European Physical Society Conference on Plasma Physics, Europhysics conference abstracts*, **35**, P4.052 (2011)
- [6]. V. Igochine, A. Gude, M. Maraschek, and ASDEX Upgrade team, *IPP-Report IPP 1/338* (2010)
- [7]. V. Weinzettl, D.I. Naydenkova, D. Sestak, J. Vlcek, J. Mlynar, R. Melich, D. Jares, J. Malot, D. Sarychev, and V. Igochine, *Nuclear Instruments and Methods Physics Results A*, **623**(2), 806 (2010).

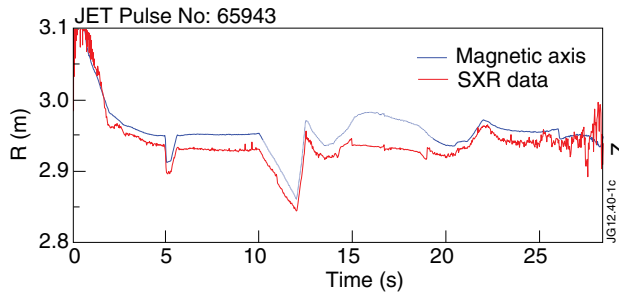


Figure 1: Comparison of the radial plasma position at JET as determined from the magnetic diagnostics (blue) and from the SXR emissivity (red). The offset is due to Shafranov shift. There is a noticeable mismatch in the interval 15s to 20s that coincides with RF heating decrease.

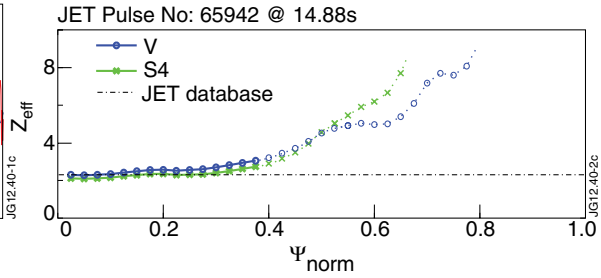


Figure 2: Effective charge derived from the SXR profiles at JET (MFR profile reconstruction). The assumption that the data correspond to plasma bremsstrahlung is valid in the plasma core only (full lines).

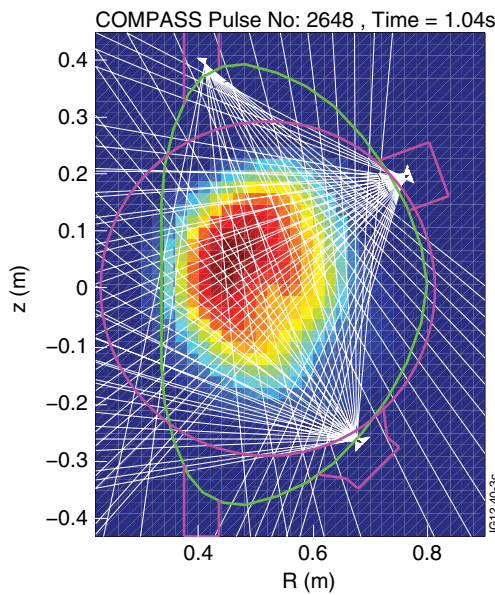


Figure 3: The AXUV emissivity reconstruction (35x45 pixels, the large circle corresponds to the zero border) of the COMPASS Pulse No: 2706 at 1.05s.

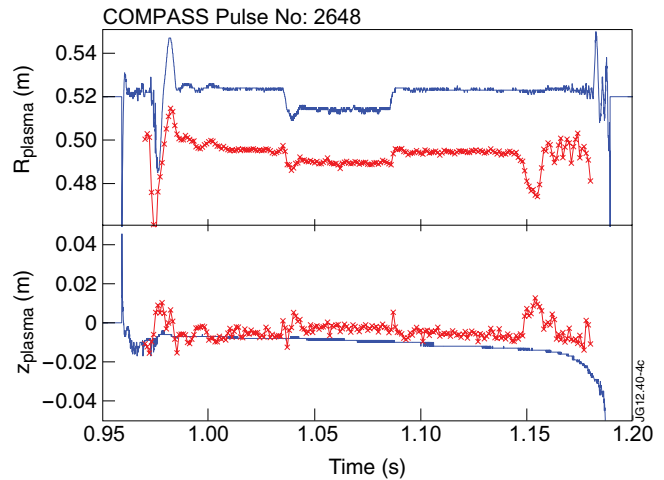


Figure 4: Plasma position in the COMPASS Pulse No: 2648 determined by magnetic diagnostics (dots) and the AXUV emissivity centre of mass (crosses).

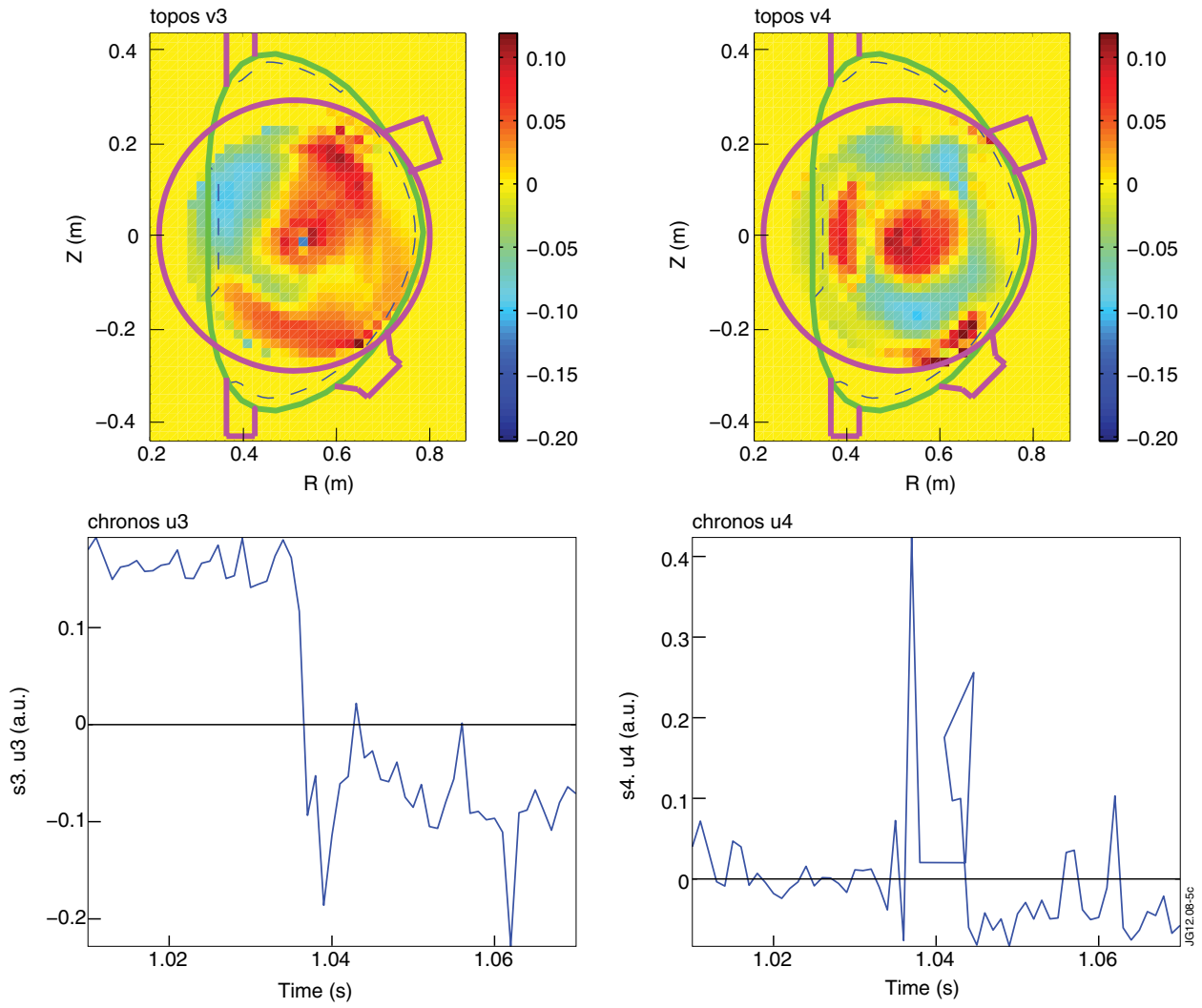


Figure 5: The SVD analysis of the AXUV emissivity evolution in COMPASS Pulse No: 2648. Notice that the third chronos remains steady after the position change, while the fourth one clearly features a temporary (perturbation) nature.